Long-range magnetic order in the Heisenberg pyrochlore antiferromagnets Gd_{2}Ge_{2}O_{7} and Gd_{2}Pt_{2}O_{7} synthesized under high pressure

X. Li, Y. Q. Cai, Q. Cui, C. J. Lin, Z. L. Dun, K. Matsubayashi, Y. Uwatoko, Y. Sato, T. Kawae, S. J. Lv, C. Q. Jin, J.-S. Zhou, J. B. Goodenough, H. D. Zhou, and J.-G. Cheng

Phys. Rev. B **94**, 214429 — Published 23 December 2016

DOI: 10.1103/PhysRevB.94.214429

Long-range magnetic order in the Heisenberg pyrochlore antiferromagnets $Gd_2Ge_2O_7$ and $Gd_2Pt_2O_7$ synthesized under high pressure

X. Li[1,2], Y. Q. Cai[1], Q. Cui[1], C. J. Lin[1], Z. L. Dun[3], K. Matsubayashi[4,5], Y. Uwatoko[4], Y. Sato[6], T. Kawae[6], S. J. Lv[1,7], C. Q. Jin[1], J.-S. Zhou[2], J. B. Goodenough[2], H. D. Zhou[3], and J.-G. Cheng[1*]

[1]Beijing National Laboratory for Condensed Matter Physics and Institute of Physics, Chinese Academy of Sciences, Beijing 100190, China

[2]Materials Science and Engineering Program, University of Texas at Austin, Austin, Texas 78712, USA

[3]Department of Physics and Astronomy, University of Tennessee, Knoxville, Tennessee, 37996, USA

[4]Institute for Solid State Physics, University of Tokyo, 5-1-5 Kashiwanoha, Kashiwa, Chiba 277-8581, Japan

[5]Department of Engineering Science, University of Electro-Communications, Chofu, Tokyo 182-8585, Japan

[6]Department of Applied Quantum Physics, Faculty of Engineering, Kyushu University, Fukuoka, 819-0395, Japan

[7]College of Physics and Engineering, Henan University of Science and Technology, Luoyang 471003, China

E-mail：jgcheng@iphy.ac.cn

Abstract

$Gd_2Sn_2O_7$ and $Gd_2Ti_2O_7$ have been regarded as good experimental realizations of the classical Heisenberg pyrochlore antiferromagnet with dipolar interaction. The former was found to adopt the Palmer-Chalker state via a single, first-order transition at $T_N \approx 1$ K, while the latter enters a distinct, partially ordered state through two successive transitions at $T_{N1} \approx 1$ K and $T_{N2} = 0.75$ K, respectively. To shed more light on their distinct magnetic ground states, we have synthesized two more gadolinium-based pyrochlore oxides, $Gd_2Ge_2O_7$ and $Gd_2Pt_2O_7$, under high-pressure conditions, and performed detailed characterizations via X-ray powder diffraction, *dc* and *ac* magnetic susceptibility, and specific heat measurements down to 100 mK. We found that both compounds enter a long-range antiferromagnetically ordered state through a single, first-order transition at $T_N = 1.4$ K for $Gd_2Ge_2O_7$ and $T_N = 1.56$ K for $Gd_2Pt_2O_7$, respectively, with the specific-heat anomaly similar to that of $Gd_2Sn_2O_7$ rather than $Gd_2Ti_2O_7$. Interestingly, the low-temperature magnetic specific heat of both $Gd_2Ge_2O_7$ and $Gd_2Pt_2O_7$ was found to follow nicely the T^3-dependence as expected for a three-dimensional antiferromagnet with gapless spin-wave excitations. We have rationalized the enhancement of T_N in terms of the reduced Gd-Gd distances for the chemically pressurized $Gd_2Ge_2O_7$ and the addition of extra superexchange pathways through the empty Pt-e_g orbitals for $Gd_2Pt_2O_7$, respectively. Our current study has expanded the family of gadolinium-based pyrochlores, and permits us to achieve a better understanding on their distinct magnetic properties in a more comprehensive perspective.

PACS numbers: 75.30.-m, 75.30.Kz, 75.40.-s

Introduction

Antiferromagnetically coupled Heisenberg spins on a pyrochlore lattice of corner-sharing tetrahedra are subjected to strong geometrical frustration.[1, 2] Theoretical investigations on such a spin system have shown that the nearest-neighbor exchange alone cannot produce long-range magnetic order for either classical or quantum spins.[3, 4] However, perturbations such as the magnetic dipole-dipole interaction, anisotropic or further-neighbor exchange interactions can lift the degeneracy of the ground-state manifold and select a unique ordered state. For example, Palmer and Chalker [5] proposed that the inclusion of long-range dipolar interaction would select a four-sublattice Néel state with an ordering wave vector $\mathbf{k} = (0\ 0\ 0)$, the so-called Palmer-Chalker (P-C) state. Because the Gd^{3+} ion ($S = 7/2$, $L = 0$) has a very small intrinsic anisotropy, the insulating $Gd_2Ti_2O_7$ (GTO) and $Gd_2Sn_2O_7$ (GSO) oxides are expected to be good approximations of the classical Heisenberg antiferromagnet on the pyrochlore lattice with dipolar interaction. Since the pioneer study on GTO in this context by Raju *et al.*,[6] the magnetic properties of these two compounds have been investigated with various experimental techniques, such as *dc* and *ac* magnetic susceptibility [6-10], specific heat [6, 7, 11], elastic and inelastic neutron scattering [12-16], electron spin resonance [17-20], Mössbauer [7, 21], and muon spin relaxation[22-24]. Besides, their interesting magnetic properties have also been the subject of several theoretical studies[25-29].

Experimentally, both compounds become magnetically ordered below ~ 1 K. However, their magnetic ground states exhibit different properties. For GSO, it undergoes a single, strongly first-order transition at $T_N = 1.0$ K into a long-range antiferromagnetically ordered ground state[7, 14], which is consistent with the theoretical prediction of the P-C state mentioned above. In striking contrast, two successive magnetic transitions at $T_{N1} \approx 1.0$ K and $T_{N2} \approx 0.75$ K were observed in GTO,[6, 7] which forms a partially ordered ground state having three out of four Gd spins within one tetrahedron ordered and the remaining one spin paramagnetic. Based on the analysis of the neutron diffuse scattering, Stewart *et al.*[13] initially proposed a 4-k magnetic structure with $\mathbf{k} = (½\ ½\ ½)$ characterized by a spatial correlation length of ~3.6 Å for the disordered spins corresponding to the nearest neighbor Gd-Gd distance. However, a very recent study on GTO by Paddison *et al.*[16] provided evidences in favor of the 1-k structure in which the disordered spins belong to different tetrahedra with a larger separation of ~ 7.2 Å. Thus, the exact magnetic structure of GTO remains an open issue. The different magnetic structures and the ordering processes between GTO and GSO are also echoed by their distinct low-energy spin excitations below T_N. The magnetic specific heat $C_m(T)$ of GSO drops exponentially below 350 mK,[11] pointing to a conventional, gapped spin-wave excitations, which was confirmed by the inelastic neutron scattering.[15] Starting from the P-C state, Del Maestro and Gingras [27] actually predicted such conventional magnons gapped by the single-ion anisotropy and dipolar interactions. In contrast, $C_m(T)$ of GTO was observed to follow the T^2-dependence down to ~100 mK,[7, 22] which is rather unconventional and suggests an unusual low-energy magnetic excitations. Based on the moun spin relaxation measurements, Yaouanc *et al.*[22] proposed that the density of

magnetic states for GTO are characterized by an upturn at low energy and a small gap varied linearly with temperature.

These side-by-side comparisons between GSO and GTO highlight the extreme sensitivity of the magnetic ground state to subtle structural changes for these highly frustrated pyrochlore antiferromagnets. The presence of theoretically predicted P-C state in GSO but not in GTO suggests that additional contributions other than the nearest-neighbor exchange and dipole-dipole interactions are at play for GTO. On the basis of a mean-field study, Wills *et al.*[14] proposed that one kind of third-neighbor exchange across the empty hexagons J_{31} is responsible for the stabilization of the 4-k structure in GTO. This proposal seems to be reasonable in that a smaller lattice constant of GTO (*i.e.* a =10.182 Å of GTO versus 10.454 Å of GSO)[7] would give rise to stronger third-neighbor exchange interactions J_{31}. In a recent theoretical investigation by Javanparast *et al*.[29], on the other hand, thermal fluctuations are argued to be responsible for the observed partially ordered 4-k state in GTO. It should be noted that GTO is prone to structural disorders. Careful treatments such as a long synthetic duration and low-temperature oxygen anneal have to be adopted in order to minimize the structural disorders,[30] which was found to have a profound impact on the magnetic properties of polycrystalline GTO samples. For example, the second transition at T_{N2} cannot be discerned in the polycrystalline samples with a high level of structural disorders. In this regard, it remains an open question whether the remaining structural disorders or the further-neighbor exchange interactions play a dominant role in determining the distinct magnetic ground state of GTO.

As pointed out by Gardner *et al*.[31], the current understanding of these Heisenberg pyrochlore antiferromagnets is still incomplete. In addition, the partial magnetic order evidenced in GTO has attracted some recent research interest.[16, 29] In order to gain more insights into these long-standing issues, we undertook in this work a detailed experimental investigation on the magnetic properties of two more gadolinium-based Heisenberg pyrochlore antiferromagnets, $Gd_2Ge_2O_7$ (GGO) and $Gd_2Pt_2O_7$ (GPO), which can be stabilized only under high-pressure and high-temperature conditions. Both compounds have been known since 1968,[32, 33] but their magnetic properties remain largely unexplored to date. Since the Gd-Gd distances are much reduced in GGO due to the smaller size of Ge^{4+}(0.53 Å) compared to Sn^{4+}(0.69 Å) and Ti^{4+}(0.605 Å), the dipole-dipole coupling and the nearest- and further-neighbor exchange interactions are expected to be enhanced accordingly. On the other hand, the presence of spatially more extended 5d orbitals for nonmagnetic Pt^{4+} ($5t_{2g}^6e_g^0$) might also influence profoundly the magnetic properties of GPO, as demonstrated in our recent work on $Er_2Pt_2O_7$ and $Yb_2Pt_2O_7$.[34] Interestingly, we found that both GGO and GPO undergo a single, strongly first-order antiferromagnetic transition with characteristic specific-heat anomaly similar to GSO, and the transition temperatures, T_N = 1.4 K for GGO and T_N = 1.56 K for GPO, are greatly enhanced with respect to that of GSO and GTO. In addition, the magnetic specific heat for both compounds was found to follow the T^3-dependence as a conventional antiferromagnet with gapless spin-wave excitations, also different from that of GSO and GTO. Although the higher T_N of GGO can be understood generally from

the viewpoint of shortened Gd-Gd distances, the observed T_N of GPO is unexpectedly high by considering only the effect of chemical pressure. Instead, we propose that it is the empty Pt-e_g orbitals that provide extra pathway for the superexchange interactions among the Gd-Gd spins. Our current study thus allows us to inspect the distinct properties of Gd-based Heisenberg pyrochlores in a more comprehensive perspective.

Experimental details

Polycrystalline GGO and GPO samples were obtained by sintering the stoichiometric mixture of Gd_2O_3 and GeO_2 or PtO_2 powers with a Kawai-type multianvil high-pressure module in the Institute of Physics, Chinese Academy of Sciences (IOP, CAS). The synthesis conditions are 7 GPa and 1000-1100 °C for GGO, and 4 GPa and 1000 °C for GPO, respectively. The high-pressure product is single phase for GGO, whereas that of GPO contains a certain amount of platinum metal and unreacted Gd_2O_3, which can be removed by solution in warm aqua regia. To facilitate the subsequent magnetic and specific-heat measurements, the obtained GPO powders were pressed into pellets and then subjected to heat treatment at 900 °C for 10 h in air at ambient pressure.

Room-temperature powder X-ray diffraction (XRD) was employed to examine the phase purity of obtained high-pressure products. We have applied the Rietveld refinements on the XRD patterns with the Fullprof program to extract the structural parameters and to evaluate the degree of site disorder in these samples. The *dc* magnetic susceptibility of GGO in the temperature range 0.5-1.8 K was measured with a superconducting quantum interference device magnetometer (Quantum Design) equipped with a home-made ^{3}He insert in the Institute for Solid State Physics, University of Tokyo (ISSP, UT).[35] All other *dc* magnetic measurements above 1.8 K were performed with a magnetic property measurement system (MPMS-III, Quantum design) in the IOP, CAS. The typical sample mass is about 30 mg for the *dc* magnetic measurements, and the data were collected after each temperature is stabilized for 5 seconds. The *ac* magnetic susceptibility measurements down to 100 mK under various magnetic fields were carried out either in an Oxford Heliox insert or a dilution refrigerator with the mutual induction method; an *ac* magnetic field of ~ 1 Oe with a fixed frequency of 317 Hz was generated in the primary coil, and the output signal across two oppositely wound secondary coils was picked up with a Standford Research SR830 lock-in amplifier. The typical sample mass is about 3-5 mg for the *ac* magnetic measurements, and the data were collected upon cooling down with a sweep rate less than 0.05 K/min for $T < 2$ K. Specific-heat measurements under zero field were carried out upon cooling down with the two-tau relaxation method in a physical property measurement system (PPMS, Quantum Design) equipped with a dilution refrigerator insert in the University of Texas at Austin. A larger sample ~ 12 mg was used for measurements above 2 K, while a smaller and thinner sample of ~ 2 mg was employed for measurements in the dilution refrigerator. We have also performed specific-heat measurements on $Gd_2Ge_2O_7$ (sample mass ~ 30 mg) under

various magnetic fields up to 9 T by using the semi-adiabatic method in the ISSP, UT. The sample was fixed to a silver platform with the GE varnish.

Results

1. Structural characterizations

The powder XRD patterns of GGO and GPO shown in Fig. 1 confirm that both samples are single phase with the cubic pyrochlore structure. These XRD patterns were refined in a cubic *Fd-3m* (No. 227) space group with the Gd atom at 16*d* (1/2, 1/2, 1/2), the Ge/Pt atom at 16*c* (0, 0, 0,), the O1 atom at 48*f* (*x*, 1/8, 1/8), and the O2 atom at 8*b* (3/8, 3/8, 3/8) site, respectively. To check the degree of site disorder, we have allowed the site exchange between Gd and Ge/Pt in the final refinements. Based on the XRD data, the degree of site mixing, *i.e.* the percentage of Ge/Pt occupying the Gd site, was found to be around 4.0(1)% for GGO and GPO. Figs. 1(a, b) illustrate the goodness of fitting for both compounds. The obtained structural parameters for GGO and GPO from Rietveld refinements are listed in Table 1 together with those of GTO and GSO for comparison.

The obtained lattice constants a = 9.9985(1) Å for GGO and a = 10.2595(9) Å for GPO agree well with the previously reported values of 9.995 Å [32] and 10.261 Å [33]. As shown in Fig. 2(a), the cubic lattice constant a increases linearly with the ionic radius (*IR*) of B^{4+} ions along the $Gd_2B_2O_7$ series (*B* = Ge, Ti, Pt, Sn), signaling a progressive increment of chemical pressure on the Gd^{3+} pyrochlore lattice by reducing the B^{4+}-ion size. It should be noted that the lattice constant of $Gd_2Pb_2O_7$ also stays nicely on the straight line of a vs $IR(B^{4+})$ despite of a high degree of site mixing (~40%).[36] This means that the chemical pressure controlled mainly by the size of B^{4+} cation is a steric effect. Thus, one has to clarify the degree of site disorder before discussing the effect of chemical pressure on the magnetic properties.

As a measure of the axial distortion along the local [111] direction for the A-site cation in the pyrochlore structure,[37] the Gd-O bond length ratio $\rho \equiv$ (Gd-O2)/(Gd-O1) in Fig. 2(a) increases generally with the *IR* of B^{4+} in the series of $Gd_2B_2O_7$ (*B* = Ge, Ti, Sn). However, a clear deviation is observed for GPO due to an anomalously short Gd-O1 bond length shown in Fig. 2(b). Very similar local structure characteristics have also been observed in $Er_2Pt_2O_7$ among the series of $Er_2B_2O_7$ (*B* = Ge, Ti, Pt, Sn).[34] These intrinsic crystallographic features of the platinum pyrochlores thus underscore the important difference of Pt^{4+} ions with respect to other nonmagnetic ions, *i.e.* the Pt^{4+} ion with spatially more extended 5d orbitals tends to squeeze the Gd-O1 bonds that are lying roughly within the same buckled plane perpendicular to the local [111] direction.[34] On the other hand, the presence of empty e_g orbitals in Pt^{4+} ($5t_{2g}^6e_g^0$ in a low-spin state within an octahedral oxygen coordination) will also influence the magnetic properties as shown below.

2. Magnetic properties

Fig. 3 (a) displays the inverse *dc* magnetic susceptibility $\chi_{dc}^{-1}(T)$ for GGO and GPO. Both show nice linear behaviors in the measured temperature range. Applications of the Curie-Weiss fitting to $\chi_{dc}^{-1}(T)$ in the temperature range 10-300 K yield an effective moment $\mu_{eff} = 8.05(1)\ \mu_B$ and a Weiss temperature $\theta_{CW} = -11.1(1)$ K for GGO, and $\mu_{eff} = 7.94(1)\ \mu_B$ and $\theta_{CW} = -8.8(1)$ K for GPO, respectively. Like in GTO and GSO, the obtained μ_{eff}s are very close to the expected value of 7.94 μ_B/Gd^{3+} for the free ion $^8S_{7/2}$ ground state of Gd^{3+}. As demonstrated in the diluted GTO,[6] the negative θ_{CW} in GGO and GPO reflects dominate antiferromagnetic interactions between the Gd^{3+} spins. As compared in Table 1, the antiferromagnetic interactions proportional to $|\theta_{CW}|$ are enhanced progressively with reducing the *IR* of B^{4+} cations as expected. (It should be noted that there are some discrepancies for the reported θ_{CW} in literatures. The θ_{CW} values for GSO and GTO listed in Table 1 came from the same report[7].) The $M(H)$ curves at 2 K increase with field and reach ~6.0μ_B under 7 T for both compounds as shown in Fig. 3(b).

In order to determine the antiferromagnetic transition temperatures for GGO and GPO, we resorted to the *dc* and *ac* magnetic susceptibility measurements at low temperatures. As shown in Fig. 3(c), the *dc* magnetic susceptibility χ_{dc} of GGO measured in the zero-field-cooling mode displays a clear cusp-like anomaly at $T_N = 1.42$ K, while the *ac* susceptibility χ_{ac} of GPO peaks out at $T_N = 1.56$ K. Both features in *dc* and *ac* susceptibilities resemble those of GSO at T_N [7, 38], confirming the occurrence of long-range antiferromagnetic transition in GGO and GPO. It should be noted that a sharp jump in the field-cooled χ_{dc} is evidenced at T_N of GSO.[7] These transition temperatures are further confirmed by the specific-heat measurements shown below. Although a higher T_N is expected for the chemically compressed GGO, the observed T_N for GPO is surprisingly high implying that other factors beyond the effect of chemical pressure play an important role as will be discussed below. Based on the obtained values of T_N and θ_{CW}, the frustration index $f \equiv |\theta_{CW}|/T_N$ is estimated to be 7.8 for GGO and 5.6 for GPO, respectively. As compared in Table 1, these f factors are reduced relative to that of GSO and GTO, especially for GPO due to the more profound enhancement of T_N.

3. Specific heat

Temperature dependence of specific heat $C(T)$ for GGO and GPO measured in a large temperature range 0.1-295 K are displayed in Fig. 4(a) in a double logarithmic scale in order to highlight the ultralow-temperature features. The $C(T)$ data of their sister compounds, GSO [7, 11] and GTO [22], are also included for comparison. As can be seen, both GGO and GPO exhibit a single, sharp specific-heat peak, resembling that of GSO rather than GTO. The transition temperatures determined from the peak are $T_N = 1.40$ K and 1.57 K for GGO and GPO, respectively, which are in excellent accordance with those determined from the magnetic susceptibility shown in Fig. 3(c). The specific-heat jump around T_N is as large as 45 and 30 J/mol-Gd K for GGO and GPO, respectively. Although these anomalies are less pronounced than that of GSO, they are much stronger than that of the best GTO ever reported [22]. Importantly,

they are higher than the mean-field value of 20.4 J/mol-Gd K for a second-order magnetic transition for $S = 7/2$,[39] suggesting a strong first-order nature of the antiferromagnetic transition as in GSO. The first-order nature is also confirmed by the presence of small thermal hysteresis in the $M(T)$ curves of GPO.[40] Another noteworthy feature in Fig. 4(a) is that the drop of $C(T)$ for GGO and GPO at the lowest temperature region is less profound as GSO [11], implying the presence of different low-energy magnetic excitations.

In order to estimate the entropy change associated with the antiferromagnetic transition and to evaluate precisely the low-energy magnetic excitations, we have obtained the magnetic specific heat $C_m(T)$ by subtracting from the measured $C(T)$ the lattice C_{lat} and the gadolinium nuclear C_{nucl} contributions. Here, we have taken the $C(T)$ of isostructural, nonmagnetic counterpart, $Lu_2Ge_2O_7$ and $Lu_2Pt_2O_7$, as the lattice standard C_{lat} for GGO and GPO, respectively, while the $C_{nucl} = 1.35 \times 10^{-4}\ T^{-2}$ was taken from literature [11]. They are also shown in Fig. 4(a). The resultant $C_m = C - C_{lat} - C_{nucl}$ and the magnetic entropy S obtained by integrating C_m/T are displayed in Fig. 4(b) and 4(c) for GGO and GPO, respectively. Since the C_{lat} and C_{nucl} are about 2 orders of magnitudes smaller than the C_m in the temperature range 0.2-1 K, any uncertainty in C_{lat} and C_{nucl} will not influence the conclusions reached below. For both cases, the entropy statures to the value very close to the expected $R\ln(8)$ for $S = 7/2$ of Gd^{3+}, where R is the ideal gas constant. As observed in many geometrically frustrated magnets, over 50% of entropy has been released above T_N for both compounds due to the presence of strong short-range spin correlations.

The magnetic specific heat C_m at $T < T_N$ provides important information about the low-lying spin excitations arising from the ordered state. Interestingly, the $C_m(T)$ of both GGO and GPO in the lowest temperature region are found to follow nicely a $C_m \propto T^3$ dependence, Fig. 4(b, c), as expected for a conventional three-dimensional antiferromagnet with gapless spin-wave excitations. In addition, a crossover to $C_m \propto T^2$ dependence takes place at ~ 0.5 K and 0.6 K for GGO and GPO, respectively. The observation of conventional 3D antiferromagnetic spin-wave excitations in GGO and GPO is surprising in view of the unusual magnetic specific heat for GTO and GSO reported in the literature [11, 22]. Earlier specific-heat measurements on GSO and GTO also evidenced an anomalous T^2-depdence just below their T_Ns. Such a T^2-depdence of C_m has been observed to hold for GTO down to 100 mK, Fig. 4(a), which has been ascribed to an unusual energy dependence of the density of states of magnetic excitation spectrum.[22] As mentioned above, on the other hand, the T^2-dependence of C_m for GSO was found to change to an exponential function, *i.e.* $C_m \propto (1/T^2)\exp(-\Delta/T)$, below 0.35 K,[11] as expected in a conventional antiferromagnet with a gapped spin-wave excitation spectrum, which has been attributed to the anisotropy due to single-ion effects and long-range dipolar interactions. The absence of spin-wave excitation gap in GGO and GPO indicated that the anisotropy plays a less important role, at least in the investigated temperature range. As discussed below, the anisotropic effect is still present in GGO and GPO, but its influence on the spin-wave excitation spectrum might be overtaken by the more strengthened superexchange interactions in GGO and GPO.

4. *T*(*H*) Phase diagram of GGO

Although the single-ion anisotropy is expected to be very small for the Gd^{3+} with $S = 7/2$ and $L = 0$, recent electron spin resonance experiments evidenced a sizable anisotropy constant with respect to the exchange and dipolar couplings due to the trigonal symmetry and higher order spin-orbit coupling.[41] As a result, the application of external magnetic field has been found to induce multiple magnetic phases in both GSO [15, 38] and GTO [30, 42]. In this study, we have also employed *dc* and *ac* magnetic susceptibility as well as specific heat to elucidate the magnetic-field-driven phase transitions in GGO.

Displayed in Fig. 5(a, b) are the temperature dependences of *dc* and *ac* magnetic susceptibilities of GGO measured below 2 K under various external magnetic fields. As seen in Fig. 5(a), in addition to the anomaly at T_N, the application of 1 T field induced a shoulder around 0.9 K, which seems to shift to below 0.6 K under 1.5 T. On the other hand, two successive anomalies appear in the $\chi_{dc}(T)$ curve under 2 T. The evolution of these field-induced anomalies can be seen more clearly from the dense $\chi_{ac}(T)$ curves in Fig. 5(b). Upon the application of magnetic field below 1.5 T, a shoulder first emerges at ~0.9 K and develops into a broad hump, which then moves to lower temperatures with further increasing magnetic field. Above 1.5 T, the anomaly at $T_N \sim 1.4$ K in $\chi_{ac}(T)$ splits into two peaks, similar to that observed in the $\chi_{dc}(T)$ curve under 2 T, and the low-temperature peak shifts to lower temperatures and smears out with increasing field to ~ 3 T. Above 3 T, another new shoulder develops below T_N and moves to lower temperatures with magnetic field, as seen in the field range below 1.5 T. At the same time, T_N is also suppressed gradually by magnetic field, Fig. 5(b). The specific-heat data shown in Fig. 5(c) further confirmed that T_N can be suppressed gradually by the external magnetic field. In accordance with the $\chi_{dc}(T)$ curve at $H = 2$ T in Fig. 5(a), the $C(T)$ data at 2 K also evidenced two successive anomalies at 1.4 and 1.2 K, respectively.

By plotting the characteristic temperatures of these above-mentioned shoulder and peak anomalies in these magnetic susceptibility and specific heat curves, we constructed a magnetic phase diagram for GGO shown in Fig. 6. Except for the low-field phase boundary below 2 T and 1.1 K, the obtained phase diagram resembles that of polycrystalline GSO [38]. There are at least four different magnetic phases that can be distinguished with increasing magnetic fields for GGO. In the case of GSO, the multiple phase transitions under magnetic field have been manifested as the change of the ratio of Bragg peak intensities.[15] Further neutron studies under magnetic fields can help to clarify the complex magnetic phase diagram of GGO.

Discussions

The rare-earth stannates $R_2Sn_2O_7$ and titanates $R_2Ti_2O_7$ are the two major material families for the experimental investigations of geometrically frustrated magnetism in the pyrochlore lattice. Although they are expected to exhibit similar magnetic behaviors for a given R^{3+} ion, in reality frequently observed are many distinct properties between them. For example, long-range

magnetic order is observed in $Er_2Ti_2O_7$ [43] and $Tb_2Sn_2O_7$ [44], but is absent in their counterparts of $Er_2Sn_2O_7$ [45] and $Tb_2Ti_2O_7$ [46]. These facts reflect the extreme sensitivity of the magnetic properties for these highly frustrated pyrochlore magnets to subtle structural perturbations controlled by a slight change of the interatomic R-R distance. In order to have a comprehensive understanding on these interesting phenomena, we have initiated investigations on the magnetic properties of the corresponding $R_2Ge_2O_7$ [47-51] and $R_2Pt_2O_7$ [34] pyrochlores that can be stabilized only under high-pressure conditions.[32, 33] Detailed characterizations of these pyrochlores and systematic comparisons with the corresponding titanates and stannates can deepen our understanding towards a unified picture.[51]

By following such a similar strategy, we have undertaken in this work an experimental study on the magnetic properties of GGO and GPO pyrochlores. The main finding of this work is that both GGO and GPO undergo a long-range antiferromagnetic transition at T_N = 1.4 K and 1.56 K, respectively, which is manifested as a single specific-heat peak like GSO rather than GTO. Although the exact magnetic structures of GGO and GPO will have to leave for the future neutron experiments on the ^{160}Gd isotopically enriched samples, a direct comparison of the specific-heat anomaly in Fig. 4(a) immediately raises the question: why is GTO so special that only it undergoes two successive transitions among the gadolinium pyrochlores?

According to the previous studies, the development of the partial magnetic order in GTO involves two steps,[13] leading to the two successive transitions. In contrast, the adoption of the P-C state in GSO is accomplished via a single, strongly first-order transition.[14] Since the major structure difference between GSO and GTO is the interatomic Gd-Gd distances, it has been generally accepted that the distinct magnetic properties of GTO arise from the contributions of further-neighbor exchange interactions.[14] In comparison with GTO, the smaller Ge^{4+} (0.53 Å) in GGO reduces considerably the Gd-Gd distances so that the further-neighbor exchange interactions are expected to be strengthened substantially, while the Gd-Gd distances are changed only slightly in GPO. Unexpectedly, neither of them shows similar two successive transitions as GTO. Instead, the presence of a single, strongly first-order transition in the specific heat of GGO and GPO highly resembles to that of GSO. These observations thus cast doubts on the current interpretations, and point to some other factors that could reconcile the observed discrepancy. One plausible factor that deserves careful scrutiny is the influence of cation site disorder or off-stoichiometry. A literature survey indeed shown that the specific-heat anomaly at the magnetic transitions of GTO, especially the lower one at T_{N2}, exhibits a large variation from sample to sample.[6, 22, 30] Thus, further studies on GTO samples with carefully controlled defect level are needed to elucidate the nature of its magnetic transitions.

Another interesting finding of the present work is the observation in both GGO and GPO of magnetic specific heat $C_m \propto T^3$ at low temperatures, which corresponds to *gapless* spin-wave excitations for a conventional three-dimensional antiferromagnet. Such a low-energy magnetic excitation spectrum is different from that of GSO [11, 27] and GTO [22], Fig. 4(a). As mentioned

above, the C_m of GTO exhibits an unconventional T^2-dependence down to 100 mK,[22] implying an unusual low-energy magnetic excitations with a gap in the density of magnetic states varying linearly with temperature. In contrast, the exponential drop of $C_m(T)$ for GSO points to rather conventional antiferromagnetic gapped spin-wave excitations.[11] In both cases, the gap has been attributed to the anisotropy arising from the single-ion effects and long-range dipolar interactions.[11, 22, 27] These effects are expected to present in both GGO and GPO, but the observed conventional magnetic specific heat indicated that the influence of anisotropy becomes less important, at least in the measured temperature region down to 100-200 mK. In the case of GGO, the reduced nearest-neighbor Gd-Gd distance and the enhanced local axial distortion, Fig. 2(a), are expected to enhance both the single-ion anisotropy and the dipolar interactions. This point is also reflected in the magnetic-field induced multiple phase transitions seen in Fig. 6. Meanwhile, the superexchange interactions should also be strengthened considerably in GGO, as reflected by the ~40% enhancement of T_N with respect to GSO and GTO. Then, the observation of gapless spin-wave excitation in GGO should be attributed to a diminished ratio of anisotropy to the superexchange interactions. This ratio is further reduced in GPO in view of the weakest local axial distortion, *i.e.* the largest ρ in Fig. 2(a), and the highest T_N among these gadolinium pyrochlores. Thus, we conclude that it is the strengthened superexchange interactions in GGO and GPO that attenuate the influence of anisotropy so as to sustain a conventional, gapless spin-wave excitation spectrum.

Finally, we discuss briefly the different mechanisms for the enhanced superexchange interactions in GGO and GPO, in which the observed T_Ns are about 40% and 60% higher in comparison with GSO and GTO. In the case of GGO, the higher T_N can be qualitatively attributed to the shorter nearest-neighbor Gd-Gd distances. However, such a chemical pressure effect cannot explain the even higher T_N of GPO. Considering the electronic configuration of Pt^{4+} ($5t_{2g}^6e_g^0$) in GPO, on the other hand, we tentatively attribute the enhancement of T_N to the extra superexchange pathways through the empty e_g orbitals of Pt^{4+} via Gd-O-Pt-O-Gd. This contribution becomes particularly prominent in GPO having the spatially more extended Pt-5d orbitals. Similar phenomenon has been observed in the A-site-order perovskite $CaCu_3B_4O_{12}$ (B = Ti, Pt),[52] in which the localized Cu^{2+} spins are coupled antiferromagnetically via the B^{4+} ions through the Cu-O-B-O-Cu pathways. In comparison with a T_N = 25 K for $CaCu_3Ti_4O_{12}$, the higher T_N = 40 K in $CaCu_3Pt_4O_{12}$ has been attributed to the stronger superexchange interactions through the empty e_g orbitals of Pt^{4+} due to the strong hybridization between Pt-5d and O-2p orbitals.[52] It is interesting to note that the enhancement of T_N by 60 % from $CaCu_3Ti_4O_{12}$ to $CaCu_3Pt_4O_{12}$ is nearly identical to that from GTO/GSO to GPO observed here. Such a coincidence could serve as another evidence to testify the above argument. But we should point out that in our recent work [34] on the XY pyrochlore antiferromagnets $Er_2B_2O_7$, in which the Er^{3+} moments lying mainly within the plan perpendicular to the local [111] direction, the observed T_N = 0.3 K for $Er_2Pt_2O_7$ is substantially lower than that of $Er_2Ti_2O_7$ (1.17 K) and $Er_2Ge_2O_7$ (1.4 K). This comparison implies that the effect of hybridization on the anisotropic exchange interactions might depend on the single-ion anisotropy.

Conclusions

In summary, the magnetic properties of cubic pyrochlores $Gd_2Ge_2O_7$ and $Gd_2Pt_2O_7$ synthesized under high pressure were studied through measurements of *dc* and *ac* magnetic susceptibility, and specific-heat measurements. Both compounds were found to undergo a long-range antiferromagnetic transition at $T_N = 1.4$ K for GGO and $T_N = 1.56$ K for GPO, respectively. The transition is manifested as a single, strongly first-order specific heat anomaly as seen in GSO rather than GTO. Their low-temperature magnetic specific heat was confirmed to follow the T^3-dependence, as a conventional three-dimensional antiferromagnet with gapless spin-wave excitations. In comparison with GSO and GTO, the observed higher T_Ns have been attributed to the reduced nearest-neighbor Gd-Gd distance in GGO and the addition of extra superexchange pathways via the empty e_g orbitals in GPO, respectively. We argued that it is the enhanced superexchange interactions in both GGO and GPO that diminish the influence of anisotropy effect as so to sustain a gapless spin-wave excitation spectrum. For a more comprehensive comparison on these dipolar Heisenberg pyrochlore antiferromagnets, neutron experiments on the ^{160}Gd isotopically enriched GGO and GPO are needed to determine the exact form of their magnetic ground state.

Acknowledgements

This work is supported by the National Science Foundation of China (Grant Nos.11304371, 11574377, 51302065), the National Basic Research Program of China (Grant No.2014CB921500), the Strategic Priority Research Program (B) and the Key Research Program of Frontier Sciences of the Chinese Academy of Sciences (Grant Nos. XDB07020100, QYZDB-SSW-SLH013), and the Opening Project of Wuhan National High Magnetic Field Center (Grant No. 2015KF22), Huazhong University of Science and Technology. HDZ and ZLD acknowledges the support of Grant No. NSF-DMR-1350002. JBG and JSZ acknowledge the support of NSF DMR (Grant No. 1122603) and the Welch Foundation (Grant No. F-1066).

Note added: During the preparation of this manuscript, we noticed that Hallas *et al.* [40] reported the synthesis and characterizations of $Gd_2Pt_2O_7$. Our results are basically consistent with each other, such as the reported $T_N \approx 1.6$ K is similar. Their magnetic specific-heat data were described in a gapped function as $Gd_2Sn_2O_7$, but our specific heat data in an extended temperature range allow us to observe a $C_m \propto T^3$ dependence.

Table 1. Comparison on the structural and magnetic properties of the cubic pyrochlores $Gd_2B_2O_7$ (B = Ge, Ti, Pt, Sn)

$Gd_2B_2O_7$	B = Ge	B = Ti	B = Pt	B = Sn
IR(B^{4+}) (Å)	0.53	0.605	0.625	0.69
a (Å)	9.9985(1)	10.182	10.2595(9)	10.454
R_{nn} [≡ ($\sqrt{2}$/4)a] (Å)	3.535	3.600	3.627	3.696
x of O1at 48f (x, 1/8, 1/8)	0.3182(3)	0.327	0.337(3)	0.335
Gd-O2 (×2) (Å)	2.165(1)	2.2045	2.2243(1)	2.265
Gd-O1 (×6) (Å)	2.535(6)	2.5185	2.467(16)	2.537
ρ [≡(Gd-O2)/(Gd-O1)]	0.854	0.875	0.902	0.893
T_N (K)	1.40	1.0, 0.74	1.56	1.0
μ_{eff}(μ_B/Gd^{3+})	8.05(1)	7.7-7.8	7.94(1)	7.96-8.06
θ_{CW} (K)	-11.1(1)	-9.9(1)	-8.8(1)	-8.6(1)
$f \equiv |\theta_{CW}|/T_N$	7.93	9.9	6.2	8.6
Reference	This work	53	This work	54

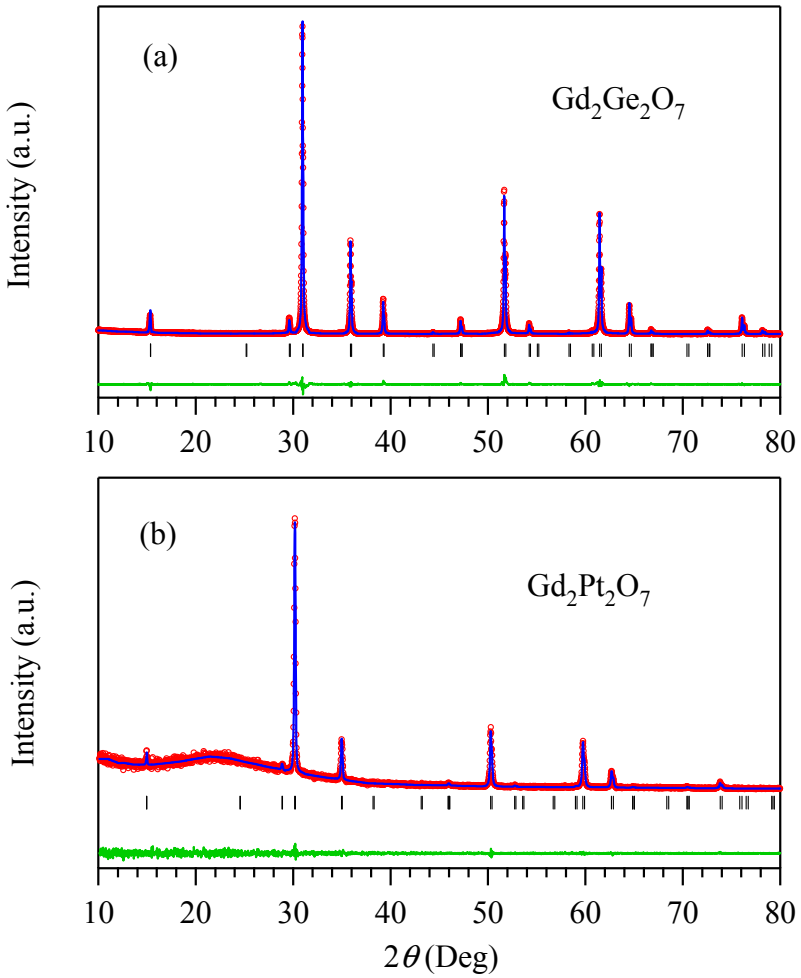

Fig. 1 (Color online) Rietveld refinements on the powder XRD patterns of (a) $Gd_2Ge_2O_7$ and (b) $Gd_2Pt_2O_7$.

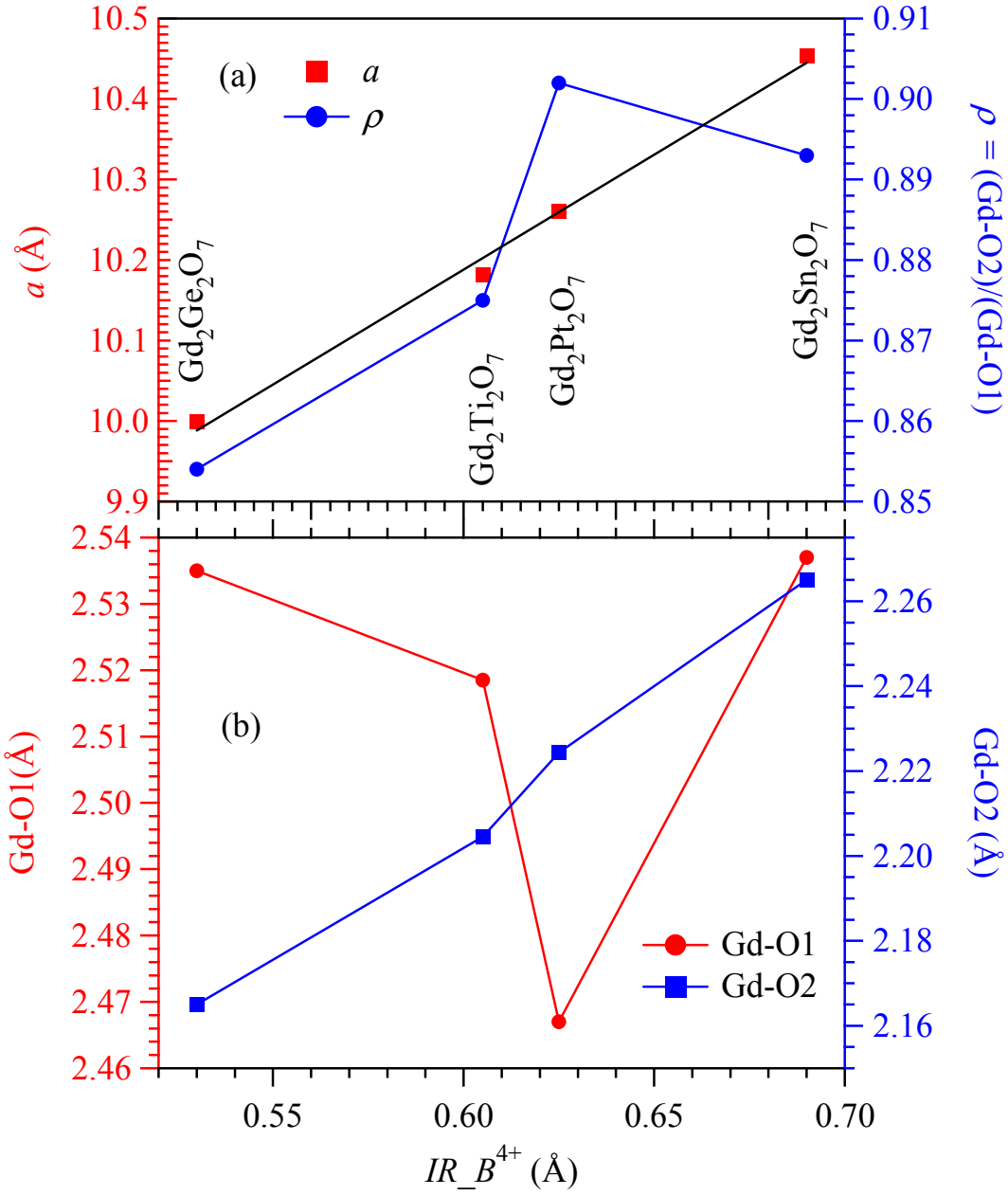

Fig. 2 (color online) (a) Lattice parameter a and the Gd-O bond length ratio $\rho \equiv$ (Gd-O2)/(Gd-O1) characterizing the axial distortion of GdO_8 polyhedra, and (b) Gd-O bond lengths in the series of $Gd_2B_2O_7$ (B = Sn, Pt, Ti, Ge) as a function of the ionic radius (IR) of the B^{4+} ions.

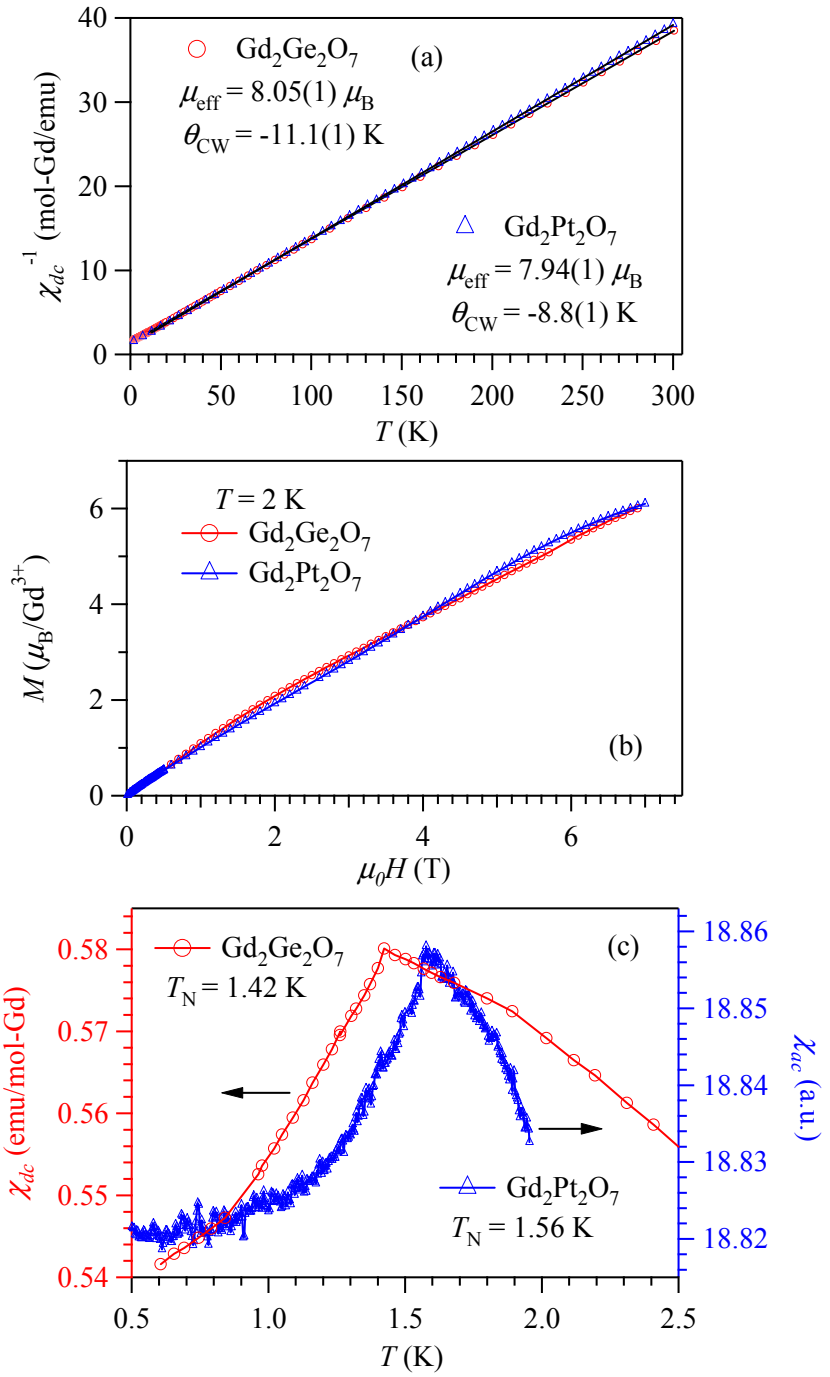

Fig. 3 (Color online) (a) Temperature dependence of the inverse *dc* magnetic susceptibility χ_{dc}^{-1} (T) of $Gd_2Ge_2O_7$and $Gd_2Pt_2O_7$ measured under H = 0.1 T in zero-field-cooling (ZFC) mode. A Curie-Weiss (CW) fitting has been applied in the temperature range 10-300K to extract the effective moment μ_{eff} and CW temperature θ_{CW}. (b) Magnetization curves at 2 K for $Gd_2Ge_2O_7$and $Gd_2Pt_2O_7$. (c) *Dc* and *ac* magnetic susceptibility for $Gd_2Ge_2O_7$ and $Gd_2Pt_2O_7$, respectively, to determine the transition temperature T_N for the long-range antiferromagnetic order.

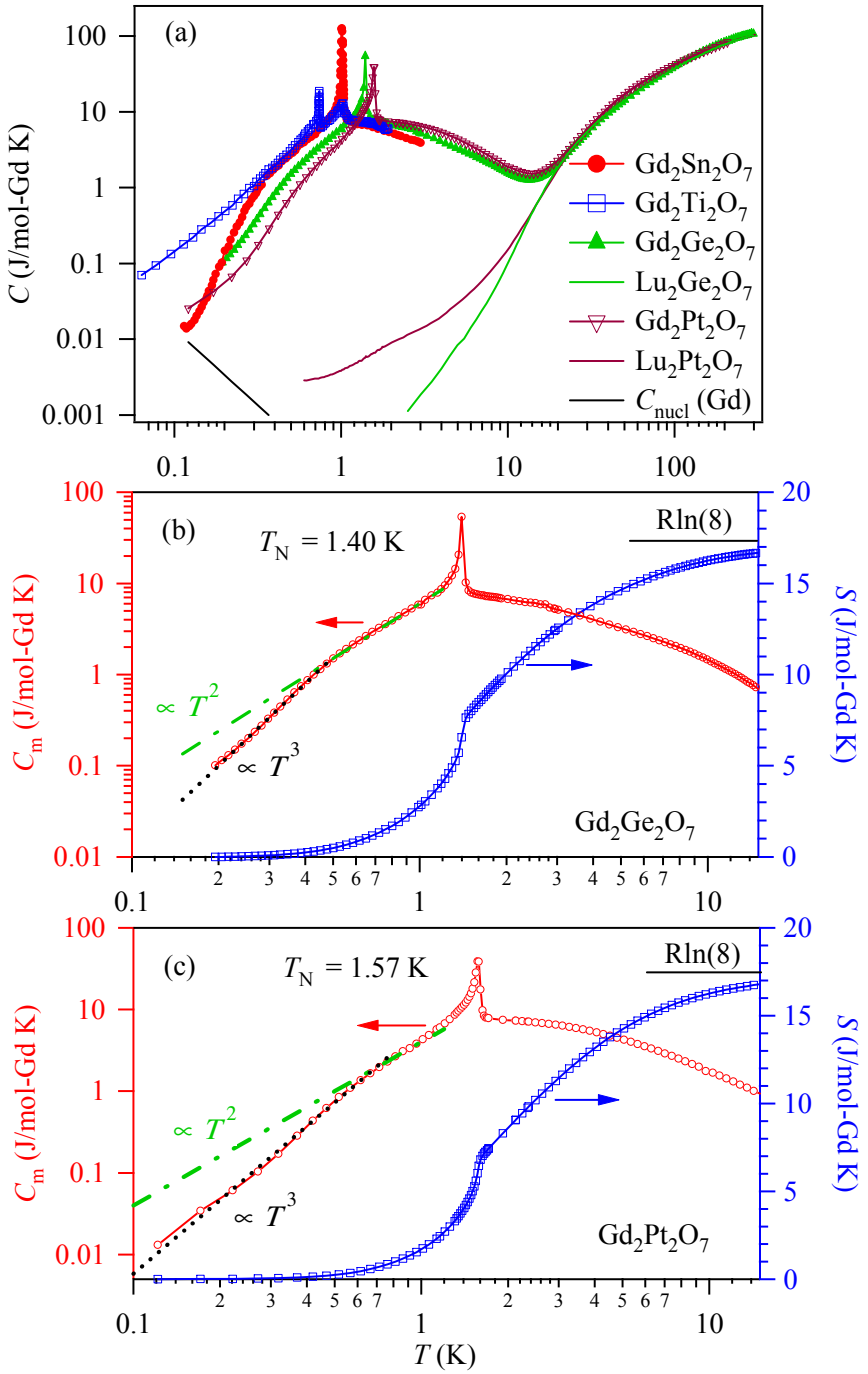

Fig. 4 (Color online) (a) Temperature dependence of specific heat $C(T)$ of $Gd_2B_2O_7$ (B = Sn, Ti, Pt, Ge) and relevant compounds. Magnetic specific heat C_m and the entropy S associated with the long-range antiferromagnetic transition for (b) $Gd_2Ge_2O_7$and (c) $Gd_2Pt_2O_7$.

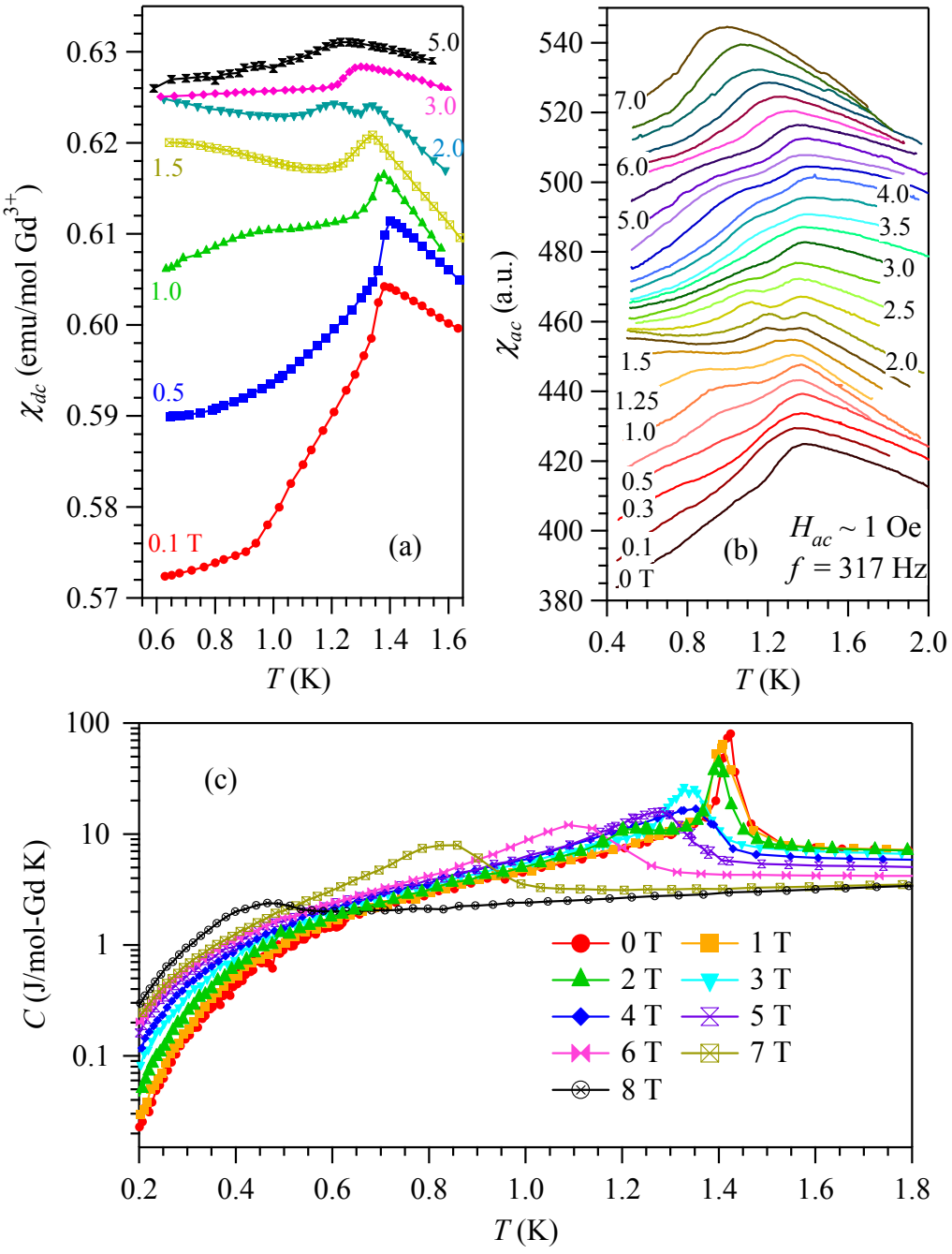

Fig. 5 (Color online) Temperature dependence of (a) *dc* magnetic susceptibility $\chi_{dc}(T)$ under different magnetic fields up to 5 T, (b) *ac* magnetic susceptibility χ_{ac}(T) under various magnetic fields up to 7 T, and (c) specific heat $C(T)$ under various fields up to 8 T for $Gd_2Ge_2O_7$.

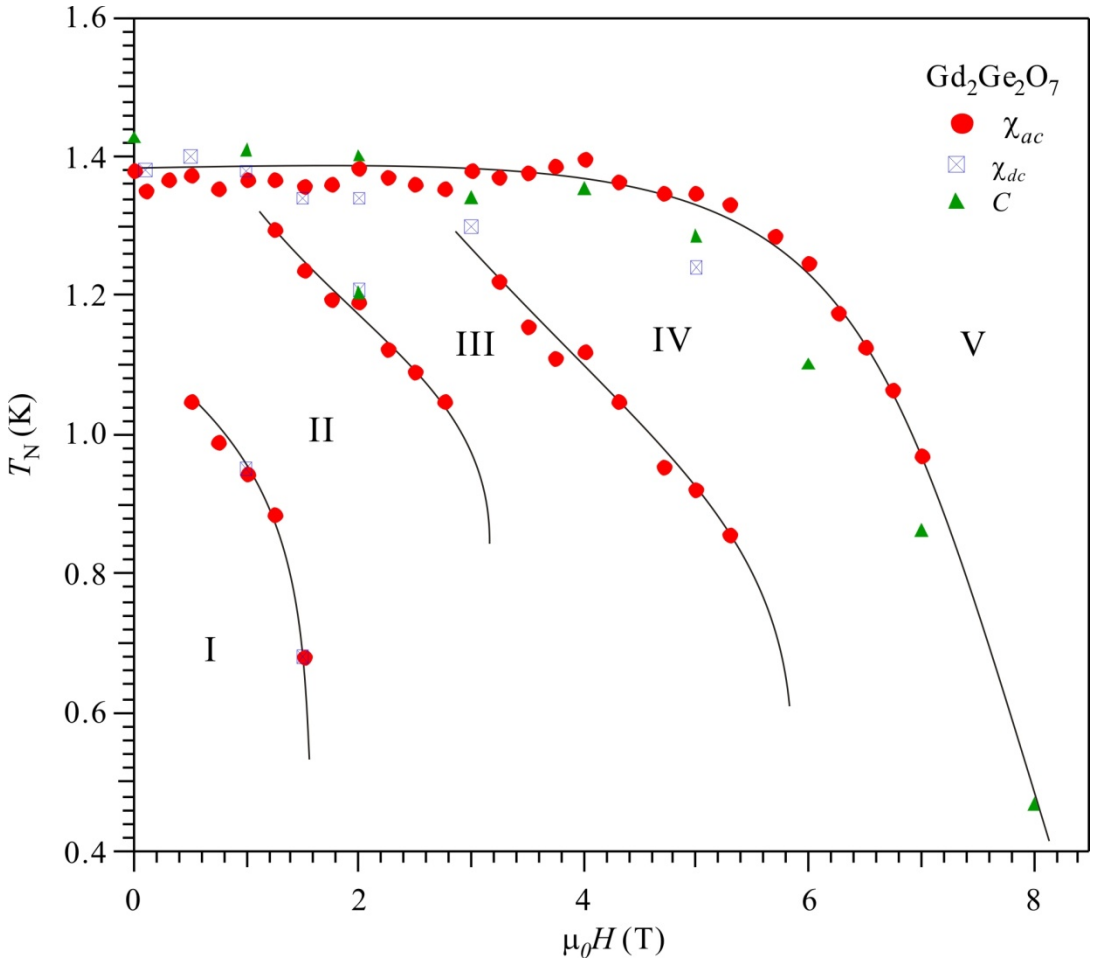

Fig. 6 (Color online) Temperature-field phase diagram of $Gd_2Ge_2O_7$ based on the field dependence of *dc* and *ac* magnetic susceptibility as well as the specific heat data shown in Fig. 5.

References

1 P. W. Anderson, Phys. Rev. **102**, 1008 (1956).

2 J. N. Reimers, A. J. Berlinsky, and A.-C. Shi, Phys. Rev. B **43**, 865 (1991).

3 R. Moessner and J. T. Chalker, Phys. Rev. Lett. **80**, 2929 (1998).

4 B. Canals and C. Lacroix, Phys. Rev. Lett. **80**, 2933 (1998).

5 S. E. Palmer and J. T. Chalker, Phys. Rev. B **62**, 488 (2000).

6 N. P. Raju, M. Dion, M. J. P. Gingras, T. E. Mason, and J. E. Greedan, Phys. Rev. B **59**, 14489 (1999).

7 P. Bonville, J. A. Hodges, M. Ocio, J. P. Sanchez, P. Vulliet, S. Sosin, and D. Braithwaite, J. Phys.: Condens. Matter **15**, 7777 (2003).

8 G. Luo, S. T. Hess, and L. R. Corruccini, Phys. Lett. A **291**, 306 (2001).

9 S. T. Bramwell, M. N. Field, J. J. Harris, and I. P. Parkin, J. Phys.: Condens. Matter **12**, 483 (2000).

[10] K. Matsuhira, Y. Hinatsu, K. Tenya, H. Amitsuka, and T. Sakakibara, J. Phys. Soc. Jpn. **71**, 1576 (2002).
[11] J. A. Quilliam, K. A. Ross, A. G. Del Maestro, M. J. P. Gingras, L. R. Corruccini, and J. B. Kycia, Phys. Rev. Lett. **99**, 097201 (2007).
[12] J. D. M. Champion, A. S. Wills, T. Fennell, S. T. Bramwell, J. S. Gardner, and M. A. Green, Phys. Rev. B **64**, 140407(R) (2001).
[13] J. R. Stewart, G. Ehlers, A. S. Wills, S. T. Bramwell, and J. S. Gardner, J. Phys.: Condens. Matter **16**, L321 (2004).
[14] A. S. Wills, M. E. Zhitomirsky, B. Canals, J. P. Sanchez, P. Bonville, P. Dalmas de Reotier, and A. Yaouanc, J. Phys.: Condens. Matter **18**, L37 (2006).
[15] J. R. Stewart, J. S. Gardner, Y. Qiu, and G. Ehlers, Phys. Rev. B **78**, 132410 (2008).
[16] J. A. M. Paddison, et al., ArXiv:1506.05045v1 (2015).
[17] S. S. Sosin, A. I. Smirnov, L. A. Prozorova, G. Balakrishnan, and M. E. Zhitomirsky, Phys. Rev. B **73**, 212402 (2006).
[18] S. S. Sosin, L. A. Prozorova, A. I. Smirnov, P. Bonville, G. Jasmin-Le Bras, and O. A. Petrenko, Phys. Rev. B **77**, 104424 (2008).
[19] A. K. Hassan, L. P. Levy, C. Darie, and P. Strobel, Phys. Rev. B **67**, 214432 (2003).
[20] S. S. Sosin, L. A. Prozorova, P. Bonville, and M. E. Zhitomirsky, Phys. Rev. B **79**, 014419 (2009).
[21] E. Bertin, P. Bonville, J.-P. Bouchaud, J. A. Hodges, J. P. Sanchez, and P. Vulliet, Eur. Phys. J. B **27**, 347 (2002).
[22] A. Yaouanc, P. Dalmas de Reotier, V. Glazkov, C. Marin, P. Bonville, J. A. Hodges, P. C. M. Gubbens, S. Sakarya, and C. Baines, Phys. Rev. Lett. **95**, 047203 (2005).
[23] S. R. Dunsiger, et al., Phys. Rev. B **73**, 172408 (2006).
[24] Y. Chapuis, P. Dalmas de Reotier, C. Marin, A. Yaouanc, A. Forget, A. Amato, and C. Baines, Physica B **404**, 686 (2009).
[25] A. G. Del Maestro and M. J. P. Gingras, J. Phys.: Condens. Matter **16**, 3339 (2004).
[26] O. Cepas, A. P. Young, and B. S. Shastry, Phys. Rev. B **72**, 184408 (2005).
[27] A. G. Del Maestro and M. J. P. Gingras, Phys. Rev. B **76**, 064418 (2007).
[28] O. Cepas and B. S. Shastry, Phys.Rev. B **69**, 184402 (2004).
[29] B. Javanparast, Z. Hao, M. Enjalran, and M. J. P. Gingras, Phys. Rev. Lett. **114**, 130601 (2015).
[30] A. P. Ramirez, B. S. Shastry, A. Hayashi, J. J. Krajewski, D. A. Huse, and R. J. Cava, Phys. Rev. Lett. **89**, 067202 (2002).
[31] J. S. Gardner, M. J. P. Gingras, and J. E. Greedan, Rev. Mod. Phys. **82**, 53 (2010).
[32] R. D. Shannon and A. W. Sleight, Inorg. Chem. **7**, 1649 (1968).
[33] H. R. Hoekstra and F. Gallagher, Inorg. Chem. **7**, 2553 (1968).
[34] Y. Q. Cai, et al., Phys. Rev. B **93**, 014443 (2016).
[35] Y. Sato, et al., Jpn. J. Appl. Phys. **52**, 106702 (2013).
[36] A. M. Hallas, A. M. Arevalo-Lopez, A. Z. Sharma, T. Munsie, J. P. Attfield, C. R. Wiebe, and G. M. Luke, Phys. Rev. B **91**, 104417 (2015).
[37] X. Li, et al., Physical Review B **89**, 064409 (2014).
[38] R. S. Freitas and J. S. Gardner, J. Phys.: Condens. Matter **23**, 164215 (2011).
[39] H. E. Stanley, *Introduction to phase transition and critical phenomena* (Oxford Unviersity Press, New York, 1971).

[40] A. M. Hallas, A. Z. Sharma, Y. Cai, T. J. Munsie, M. N. Wilson, M. Tachibana, C. R. Wiebe, and G. M. Luke, Phys. Rev. B **94**, 134417 (2016).
[41] V. N. Glazkov, M. Zhitomirsky, A. I. Smirnov, C. Marin, J. P. Sanchez, A. Forget, D. Colson, and P. Bonville, J. Phys.: Condens. Matter **19**, 145271 (2007).
[42] O. A. Petrenko, M. R. Lees, G. Balakrishnan, and D. McK Paul, Phys. Rev. B **70**, 012402 (2004).
[43] J. D. M. Champion, et al., Phys. Rev. B **68**, 020401(R) (2003).
[44] I. Mirebeau, et al., Phys. Rev. Lett. **94**, 246402 (2005).
[45] P. M. Sarte, H. J. Silverstein, V. W. B. T. K., J. S. Gardner, Y. Qiu, H. D. Zhou, and C. R. Wiebe, J. Phys.: Condens. Matter **23**, 382201 (2011).
[46] J. S. Gardner, et al., Phys. Rev. Lett. **82**, 1012 (1999).
[47] H. D. Zhou, et al., Nat. Comm. **2**, 478 (2011).
[48] H. D. Zhou, et al., Phys. Rev. Lett. **108**, 207206 (2012).
[49] A. M. Hallas, et al., Phys. Rev. Lett. **113**, 267205 (2014).
[50] Z. L. Dun, et al., Physical Review B **89**, 064401 (2014).
[51] Z. L. Dun, et al., Physical Review B **92**, 140407(R) (2015).
[52] I. Yamada, et al., Inorg. Chem. **49**, 6778 (2010).
[53] Y. Tabira, R. L. Withers, L. Minervini, and R. W. Grimes, J. Solid State Chem. **153**, 16 (2000).
[54] B. J. Kennedy, B. A. Hunter, and C. J. Howard, J. Solid State Chem. **130**, 58 (1997).